Biochimica et Biophysica Acta, 471 (1977) 227—242

BBA 77861

VOLTAGE-INDUCED PORE FORMATION AND HEMOLYSIS OF HUMAN ERYTHROCYTES

KAZUHIKO KINOSITA, Jr. and TIAN YOW TSONG *

Department of Physiological Chemistry, The Johns Hopkins University School of Medicine, Baltimore, Md. 21205 (U.S.A.)

(Received June 17th, 1977)

Summary

Isotonic suspensions of human erythrocytes were exposed to single electric pulses of intensity at a few kV/cm and duration in microseconds. Upon pulsation, the cell membranes became permeable to Na^+ and K^+, and the erythrocytes eventually hemolysed through the colloid osmotic effect of hemoglobin. The enhanced permeability is attributed to the formation of pores in the cell membranes. These pores are formed within a fraction of a microsecond, once the transmembrane potential induced by the applied electric field reaches a critical value of 1.0 V. Increased field intensity and pulse duration, or pulsation at low ionic strengths all expand the pore size, leading to an accelerated hemolysis reaction. In contrast to this expansion process, the initial step of pore formation is governed solely by the magnitude of the transmembrane potential: the critical value of the potential stays essentially constant in media of different ionc strengths, nor does it change appreciably with varying pulse duration. An abrupt increase in membrane permeability at a transmembrane potential around 1 V has been observed in many cellular systems. It is suggested that a similar mechanism of pore formation may apply to these systems as well.

Introduction

Exposure of a cell suspension to an electric pulse of intensity at a few kV/cm to 30 kV/cm, and of duration in the ms range, in many cases results in the lysis of the cells [1—5]. Studies from several laboratories have indicated that the lysis is due to a large transmembrane potential induced by the applied electric field [1,2,5]. In the case of human erythrocytes, a transmembrane potential of approx. 1 V, which corresponds to an applied field of 2.5 ± 0.5 kV/cm, causes hemolysis in 50% of the treated cells [5].

* To whom correspondence should be addressed.

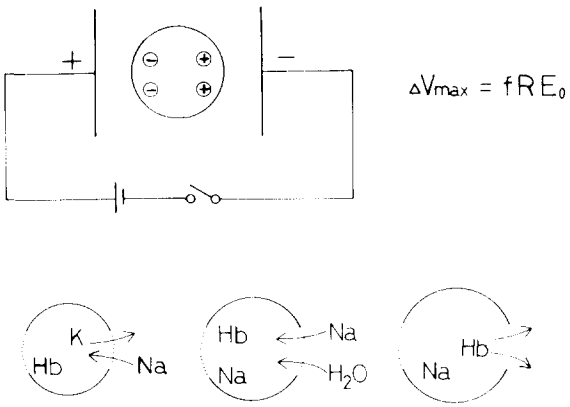

Fig. 1. Mechanism of the voltage-induced hemolysis. When an erythrocyte in an isotonic NaCl solution is exposed to a uniform electric field E_0 between a parallel pair of electrodes, the intracellular ions move along the field until they are held back by the cell membrane. The accumulation of ions on the surfaces of the membrane generates a large transmembrane potential around the two loci opposing the electrodes. The maximal value of the potential ΔV_{max} is given by the equation in the figure, where R is the largest semi-axis of the cell and f is the geometric factor having a value around 1 (see Appendix I). When the transmembrane potential reaches a critical value of approximately 1 V, it creates pores in the membrane, which remain open after the removal of the applied field. Thus, the intracellular potassium leaks out into the medium and the external sodium enters the cell. Continuous influx of sodium (and chloride) toward equilibrium is accompanied by water influx, so as to maintain the osmotic balance, resulting in a gradual swelling of the cell. When the cell volume reaches a limit, the erythrocyte punctures and releases hemoglobin.

In a previous paper [5], we have shown that the primary effect of the electric pulsation is an increase in the membrane permeability and that the lysis is a secondary effect. Thus, human erythrocytes treated with the voltage pulse were found to be much more permeable to Na^+ and K^+ than untreated cells. Permeation of these ions toward equilibrium together with the excess osmotic pressure due to the presence of hemoglobin inside led to the swelling and the eventual hemolysis of the red cells (see Fig. 1). This type of cell lysis is known as colloid osmotic lysis [6,7].

Furthermore, the enhanced permeability of the pulse-treated erythrocytes to various substances has been shown to decrease with increasing size of permeant molecules, reaching a virtual impermeability at a critical size [8]. Thus, it was suggested that the electric pulsation creates or opens up pores in the cell membranes. The size of these pores could be varied in a controlled manner: increase in the field intensity, the pulse duration, or decrease in the ionic strength all resulted in the formation of larger pores. Incubation at 37°C annealed these pores; under certain conditions, the leaky membranes were resealed while the cells were prevented from lysis. By this procedure, foreign molecules such as sucrose have successfully been incorporated into the resealed, but otherwise intact, erythrocytes.

A more detailed study of the voltage-induced hemolysis will reveal the molecular mechanism of the pore formation, affording a further insight into the structure and functions of biological membranes. The development of the voltage-pulsation technique would also offer a convenient means for altering intracellular compositions; introduction of the pores of adequate size would

allow the incorporation of desired molecules into apparently intact cells.

Here we have undertaken both equilibrium and kinetic measurements of the voltage-induced hemolysis under a wide range of experimental conditions. It will be shown that the hemolysis and the pore formation are fully coupled events. Thus the final extent of hemolysis allows the estimation of the fraction of total cells pierced with the pores, whereas the rate of hemolysis reflects the size of these pores. The experimental results indicate a two-step mechanism for the pore formation, where the initial penetration and the subsequent widening of the pore are governed by different factors.

Materials and Methods

Fresh human blood was obtained from healthy young adults by venipuncture in the presence of heparin. Erythrocytes were washed three times by centrifugation at $1000 \times g$ for 10 min with a solution containing 150 mM NaCl and 7 mM sodium phosphate buffer, pH 7.0; buffy coats were carefully removed. Packed cells were then resuspended in a "pulsation medium" and kept at 0—4° C until just prior to the pulsation. In most experiments, the erythrocytes treated with an electric pulse were immediately mixed with a large volume of "lysing medium", in which the hemolysis reaction was allowed to proceed. Both pulsation and lysing media were mixtures at various ratios of the above NaCl solution and a 272 mM sucrose solution. (Both solutions have approximately the same osmolality, 300 milliosmolal, which was supposed to be isotonic.) Hereafter, the composition of a medium will be denoted by the volume ratio of the two solutions.

The electric pulsation was performed with a device already described [5]. An erythrocyte suspension was placed between a parallel pair of stainless steel electrodes and a single square-wave pulse (rise and fall times approx. 50 ns) was applied after equilibration at room temperature (25 ± 2°C). A dual-trace storage oscilloscope recorded the voltage and current waveforms simultaneously, from which the field intensity and the current density were estimated.

In equilibrium studies, erythrocytes suspended in a pulsation medium at 1% v/v was treated with an electric pulse, and an aliquot of 40 μl was immediately mixed with 2.0 ml of a lysing medium. (In potassium release experiments, a 20% v/v suspension was pulsated, and an aliquot of 100 μl was mixed with 900 μl of a lysing medium.) The suspension was kept at room temperature for 15—20 h with occasional mixing and at the end centrifuged at $12000 \times g$ for 5 min. The extent of hemolysis was estimated from the absorption at 410 nm of hemoglobin in the supernatant; the value for 100% hemolysis was obtained by hypotonic hemolysis in water. The amount of potassium released into the medium was determined by a flame photometer (National Instrument Laboratories) using Li_2SO_4 as internal standard. In experiments where intracellular cation content was examined, erythrocytes were pulsated at 20% v/v and then sucked into microhematocrit tubes. The samples were mixed occasionally by inversion of the tubes and finally centrifuged at $5000 \times g$ for 10 min. Measured portions of the supernatant and the pellet corresponding to unlysed cells were cut out, dissolved in Li_2SO_4, and analyzed by the flame photometer.

In kinetic studies, the extent of hemolysis was monitored by turbidity mea-

surements. Erythrocytes were pulsated at 1% v/v and, after 1.0 min, an aliquot of 40 μl was drawn and added to 2.0 ml of a lysing medium in a cuvette placed in a GCA/McPherson double-beam spectrophotometer. The suspension was continuously agitated with a small magnetic stirrer tip and the change in the turbidity at 700 nm was recorded against time. Temperature was controlled at 25 ± 1°C. Under these conditions, the turbidity was found to be roughly proportional to the number of unlysed cells; control experiments showed that the change in neither cell volume (medium tonicity varied) nor cell shape (an echinocyte-inducing agent 1-anilino-8-naphthalene sulfonate [9] added) affects the turbidity appreciably (see also Fig. 2). Time for 50% hemolysis, therefore, was determined as the time when the turbidity decreased to one half that of the untreated cells. Kinetics of potassium release was measured in the same way as in the equilibrium studies.

Results

Time courses of hemolysis at different field intensities

Fig. 2 shows typical time courses of the voltage-induced hemolysis. The ordinate, the turbidity of the whole suspension, is roughly proportional to the number of unlysed cells. It is clear that the increase in the field intensity markedly accelerates the homolysis reaction, and that an electric field greater than approx. 3 kV/cm is required for a complete hemolysis. (In all four curves shown in the figure, the homolysis reaction ceased before 800 min; turbidity values did not change over the next 20 h.) It should be emphasized that the curves presented here do not represent the time courses of hemoglobin release from individual cells. As noted previously [5], hemoglobin escapes from a cell within some 10 s once the cell punctures after swelling. The gradual decrease in the turbidity results from successive hemolysis of different cells over a period of time. Thus, the second curve from top, for example, reads, that of the eryth-

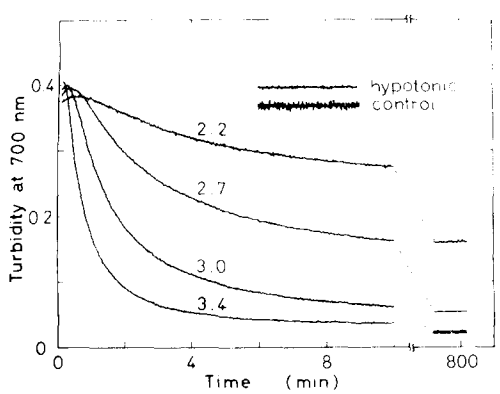

Fig. 2. Time courses of the voltage-induced hemolysis at different field intensities. Washed human erythrocytes suspended at 1% v/v in a 10% NaCl/90% sucrose isotonic mixture were treated with a 20 μs pulse of indicated intensities (kV/cm). After 1.0 min, an aliquot of the treated suspension was added to 50 vols. of isotonic NaCl solution, in which hemolysis was monitored by a decrease in the turbidity. Time zero refers to the moment of the addition. Control denotes an isotonic NaCl suspension of untreated cells; hypotonic refers to untreated cells in 180 milliosmolal NaCl. Temperature was 25° C.

rocytes treated with a 2.7 kV/cm pulse, 50% underwent hemolysis by 7 min and 10% remained unlysed at 800 min.

As is seen in the two traces on the upper-right, untreated erythrocytes swollen in a hypotonic medium gave slightly greater turbidity over control. Thus, the small hump in the left curves reflects the swelling of the pulse-treated cells prior to hemolysis [5]. The control also shows that normal biconcave erythrocytes present a higher noise level in the turbidity curve because the cells tend to align along the turbulent flows created by the stirrer [10]. Absence of prominent noise in other curves suggests that the pulse treatment immediately transforms the cells into more of less spherical shapes. In fact, Tsong and Kingsley [3] have observed that erythrocytes assume the shape of crenated sphere (echinocyte III) shortly after the voltage pulsation.

Ionic leakage at equilibrium

The previous paper [5] has shown that the extent of hemolysis, when measured after the reaction ceases, depends sigmoidally on the applied field intensity as is seen in the dashed curve of Fig. 3. Hemolysis requires an applied field intensity of 2.5 ± 0.5 kV/cm, being consistent with the result in Fig. 2. Almost identical hemolysis curves are obtained irrespective of the ionic strength of the pulsation medium, or of the current density. This independence in current excludes the rapid temperature jump of the medium as a source of hemolysis, and has led us to conclude that the hemolysis is due to a field-dependent effect, most probably the field-induced transmembrane potential.

Solid curves in Fig. 3 give the average cation composition of the pulse-treated erythrocytes versus field intensity. The data were taken 1 h after pulsation; by this time, less than 15% of the total cell population hemolysed for field intensi-

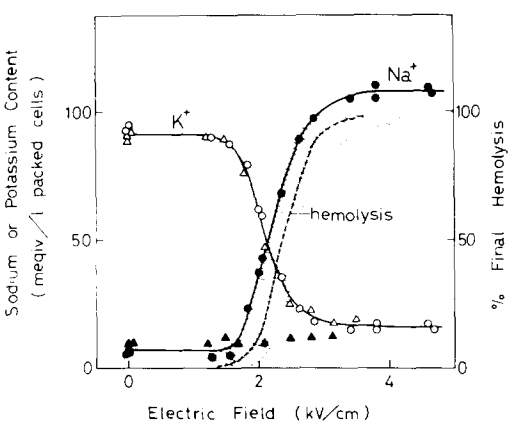

Fig. 3. Cation compositions of the pulse-treated erythrocytes. Erythrocytes suspended at 20% v/v in either isotonic NaCl (circles) or 10% NaCl/90% sucrose isotonic mixture (triangles) were treated with a 20 μs pulse of various intensities. The suspension was kept at room temperature (25 ± 2°C) for 1 h and finally spun down in a microhematocrit tube. A portion of the pellet that consists of unlysed cells was flame-analyzed for their sodium and potassium contents. The values obtained were corrected for an extracellular volume of 5% estimated as [^{14}C]sucrose accessible space. The hemolysis curve is adapted from ref. 5; the original data (pulse duration 20 μs, relative NaCl content in pulsation media 3 to 100%, lysing medium 100% NaCl, measured 20 h after pulsation) are scattered within the shaded region.

TABLE I

TIMES FOR 50% HEMOLYSIS IN DIFFERENT COMBINATIONS OF PULSATION AND LYSING MEDIA

Erythrocytes in pulsation medium were treated with a 3.7 kV/cm, 20 μs pulse and, after 1.0 min, they were transferred into a large volume of lysing medium. Hemolysis times, counted from the moment of the transfer, were determined from turbidity measurements described in Fig. 2. All media were isotonic mixture of NaCl and sucrose. Temperature was controlled at 25 ± 1°C. The values are averages of 2—4 independent measurements, the maximum variation being 50%.

Relative NaCl content in pulsation medium (%)	Time for 50% hemolysis (min)					
	Relative NaCl content in lysing medium (%)					
	100	90	70	30	10	3
100	230	>1000				
90	200	>1000				
70	210	1000	>1000			
30	13	75	230	380		
10	0.6	1.0	4	13	19	33
3	<0.2	0.2	0.3	2.4	3.5	8

ties less than 4 kV/cm (circles: medium isotonic NaCl), or 2.5 kV/cm (triangles: 10% NaCl/90% sucrose isotonic mixture). In other words, the cation content shown are those in a prelytic stage. The extent of the ionic leakage, however, remained the same for the next 10 h. The loss of potassium from unlysed cells during this period was small (aprox. 10%) and the same for all samples including the untreated control.

The figure shows that the loss of intracellular potassium and the concomitant gain of sodium occur at almost the same field intensity that induces hemolysis. The slight discrepancy, the apparent shift of the hemolysis curve toward higher field intensity, is attributed to the spontaneous resealing which proceeds slowly at 25°C [8]. In fact, the hemolysis data are scattered in the shaded area in such a manner that those corresponding to low ionic strengths, where the hemolysis reaction is fast (see Table I), lie close to the low-field edge. Ionic leakage, on the other hand, occurs within minutes under these conditions [5], and is free from the effect of resealing. Thus, the hemolysis and the ionic leakage are fully coupled events: the voltage-induced lysis is always preceded by the cation exchange, and the ionic leakage is always (unless forestalled by the resealing) followed by hemolysis. This supports, among others, the contention that the voltage-induced hemolysis is colloid osmotic in nature [5].

The fact that the leakage curves are identical for the high and low ionic conditions (circles and triangles) indicates that the initial process of the pore formation is independent of the ionic strength of the pulsation medium: pores are created once the field intensity exceeds a critical value of approximately 2.2 kV/cm, regardless of the salt concentration. As will be shown below, however, the size of the pores is strongly affected by the ionic strength.

Effect of medium composition on the rate of hemolysis

Colloid osmotic hemolysis occurs as a result of swelling, which in turn is

caused by the penetration of solutes toward equilibrium [6,7]. Thus, the rate of hemolysis is determined essentially by two factors: the permeability of membranes to the solutes, and the concentration of the solutes in the medium.

The rate of hemolysis in various media was estimated from kinetic measurements similar to those in Fig. 2. A wide range of NaCl/sucrose ratios in both pulsation and lysing media was tested under the same pulse intensity of 3.7 kV/cm and duration of 20 μs. Table I lists the time by which 50% of the treated cells hemolysed under a given set of conditions; in other words, it is the time at which a median cell underwent hemolysis.

In the first column, lysing media contained only NaCl (and a small amount of phosphate buffer); therefore, the hemolysis times reflect the permeability of the treated membranes to NaCl. It is evident that the pulsation at lower ionic strengths yields membranes of greater permeability. Presumably, the electrostatic repulsion between charged groups widens the pores. On the other hand, inclusion of sucrose in lysing media retarded hemolysis, suggesting a much slower permeation of sucrose than NaCl. In fact, when the lysing medium contains both NaCl and sucrose, the equilibrium partition of NaCl across the cell membranes is first established, resulting in the shrinkage of the cells, and then the gradual entry of sucrose re-expands the cells, leading to the lysis [5]. The slower hemolysis toward right in the table is explained by the larger uptake of sucrose required for hemolysis. In the top two rows, in particular, the presence of sucrose almost completely blocked the hemolysis. Tracer experiments have demonstrated [5] that sucrose does not penetrate under these conditions. Thus the presence of sucrose counterbalances the excess osmotic pressure of hemoglobin inside the cells.

The effect of pulse duration on the critical field intensity

All the data presented so far have been concerned with a typical pulse duration of 20 μs. In order to examine the effect of pulse duration, erythrocytes in a 10% NaCl/90% sucrose medium were treated with single pulses of various durations and subsequently transferred into an isotonic NaCl solution; the low ionic strength in the pulsation medium was chosen because the rapid reaction (see Table I) would minimize the complication due to the spontaneous resealing.

The extent of hemolysis measured 20 h after the pulsation is plotted in Fig. 4a against the log of field intensity. The hemolysis curves for different pulse durations are almost congruent with each other, showing an approximately 1.5-fold span in field intensity for each pulse duration. The amount of potassium released by 20 h gave a similar set of curves, as shown in Fig. 4b, except the fact that those for short pulses were shifted toward lower field intensities as compared to the hemolysis curves. This discrepancy again is due to the spontaneous resealing; hemolysis reaction is very slow for pulses shorter than 5 μs (see Table II).

Fig. 5 gives the critical field intensity $E_{1/2}$, at which 50% of the erythrocytes either hemolyse or release potassium, against pulse duration. As is mentioned above, the increase in $E_{1/2}$ for hemolysis at pulse durations shorter than 5 μs is due to the resealing. On the other hand, the rise of $E_{1/2}$ for ionic leakage at approximately 1 μs is real, although even the potassium release is very slow for

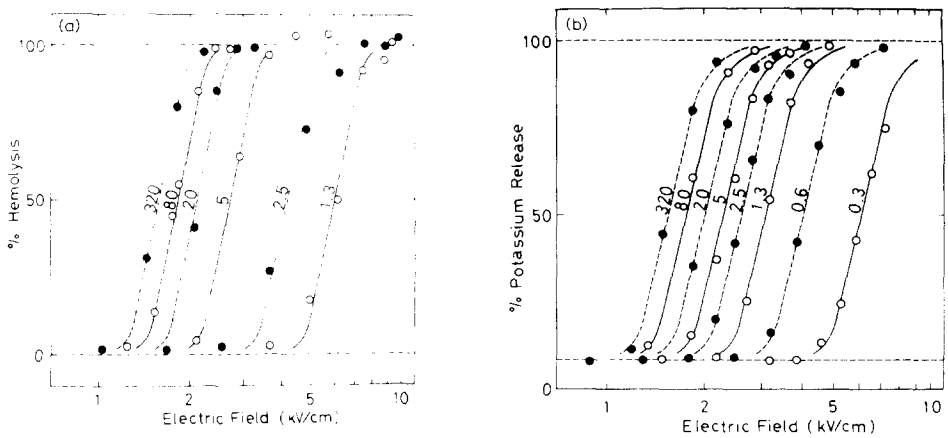

Fig. 4. The extent of hemolysis (a) and potassium release (b) at different pulse durations. Erythrocytes suspended in 10% NaCl/90% sucrose isotonic mixture were treated with an electric pulse of various intensities with indicated durations (μs). The cells were immediately transferred into isotonic NaCl solution and kept for 20 h at 25 ± 2°C with occasional mixing. After 20 h, the suspension was centrifuged and the supernatant was analyzed for its hemoglobin (absorption at 410 nm) or potassium (flame photometry) contents. 100% values were obtained by hypotonic lysis. In b, the dashed line at the bottom denotes the level of untreated cells (8%).

pulse durations less than 1 μs (half time is 1 h under a pulse of 0.3 μs at 6.2 kV/cm) and is affected somewhat by the resealing. When the lysing media were kept at 4°C, where resealing is virtually negligible [8], $E_{1/2}$ for potassium release was shifted to slightly lower values, as is shown by the closed circles in Fig. 5, but the basic feature remained the same. At 4°C, under the treatment with a 0.3 μs, 5.5 kV/cm pulse, 32% of cellular potassium leaked out by 1 h and 58% by 20 h; the amount released between 20 and 70 h (5%) was approximately one half that from untreated control (9%), indicating that one half of

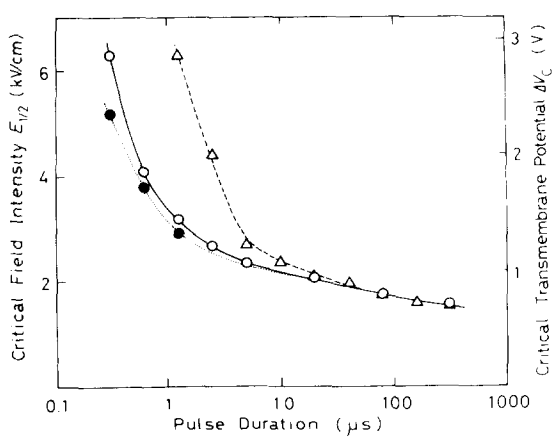

Fig. 5. The critical field intensities for hemolysis (triangles) and potassium release (circles) at different pulse durations. Left ordinate indicates the field intensity corresponding to the midpoint of the curves in Fig. 4. Closed circles were obtained from experiments similar to Fig. 4b except that the lysing medium was kept at 4°C. Right ordinate was calculated from Eqn. 2 in text.

TABLE II

TIMES FOR 50% HEMOLYSIS AT DIFFERENT PULSE DURATIONS

See Table I for details.

Field intensity (kV/cm)	Pulsation medium (% NaCl)	Lysing medium (% NaCl)	Time for 50% hemolysis (min)							
			Pulse duration (μs)							
			2.5	5.0	10	20	40	80	160	320
5.4	100	100	510	250	135	53	17	6.1	2.6	1.1
4.1	10	100	>1000	8.4	0.3	0.3	1.6	2.0	1.2	0.5
4.1	10	10	>1000	160	12	10	68	86	79	46

the pulse-treated cells are intact under this condition and that the leakage from the affected half is complete by 20 h.

Fig. 5 shows that $E_{1/2}$ is essentially independent of pulse duration above 1 μs; note that the abscissa is in the log scale. This is another evidence that the pore formation, or hemolysis as the result, is not due to the temperature-jump of the medium, the magnitude of which being proportional to the pulse duration. As will be discussed later, the rise of $E_{1/2}$ at about 1 μs is explained by the effect of membrane capacitance.

The rate of hemolysis at different pulse durations

Although the duration of pulse has little effect on the critical field intensity, it drastically influences the rate of hemolysis as is shown in Table II. When both pulsation and lysing media were isotonic NaCl solutions, 2-fold increase in pulse duration accelerated the hemolysis reaction about 2.5-fold (row 1). Sustained electric field appears to widen the pores. Still larger effect was observed when the ionic strength of the pulsation medium was decreased to 1/10 (rows 2 and 3): hemolysis by a 10 μs pulse was more than 10 times faster than that by a 5 μs pulse. Further increase in pulse duration, however, slowed down the reaction. This anomalous result was fully reproducible. The fact that the slowing down around 80 μs was observed in 10% NaCl/90% sucrose medium as well as in isotonic NaCl suggests slower permeation of both NaCl and sucrose at these pulse durations. Preliminary measurements of prelytic volume change in 10% NaCl/90% sucrose medium also confirmed that the initial shrinkage due to the efflux of potassium as well as the following swelling due to the influx of sucrose are much slower when treated with 40 or 80 μs pulse than with 10 or 20 μs pulse. Thus, prolonged pulsation at low ionic strengths appears to cause a shrinkage of the once-opened pores. More complete account of this anomalous phenomenon awaits further investigation.

Discussion

The critical transmembrane potential

When a cell in suspension is exposed to a high electric field between a pair of parallel electrodes, the ions inside the cell will move along the field until they are held back by the cell membrane whose conductivity is several orders of

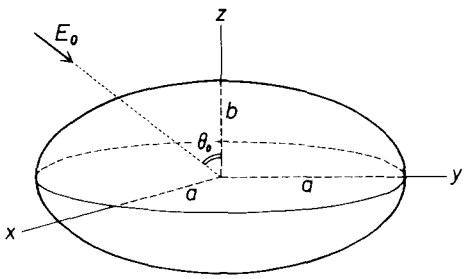

Fig. 6. A spheroidal cell with principal semi-axes a and b exposed to a uniform electric field E_0.

magnitude smaller than that of the internal fluid [7,11]. The accumulation of ions on the surfaces of the membrane will generate a large transmembrane potential, which is maximal around the two loci opposing the electrodes (see Fig. 7 in Appendix). The pore formation in erythrocyte membranes is considered to be due to this transmembrane potential [5].

If the shape of the cell is approximated by a spheroid with principal semi-axes a and b (the symmetry axis is taken as b; see Fig. 6), the maximal transmembrane potential ΔV_{max} induced by an externally applied electric field E_0 is calculated as (Appendix I)

$$\Delta V_{max} = f(\nu, \theta_0)\, RE_0 \tag{1}$$

where R is the largest semi-axis (i.e. $R = a$ for an oblate, and $R = b$ for a prolate) and f is a geometric factor which depends on the axial ratio $\nu = b/a$ and the angle θ_0 between the symmetry axis b and the direction of the field E_0 (see Fig. 6). In the case of a sphere, the factor f takes a constant value of 1.5 [4].

By applying Eqn. 1 to the data in Figs. 3 and 4, we can estimate the critical transmembrane potential ΔV_c at which the pores are formed in human erythrocyte membranes. Before attempting it, however, we first focus on the span of the curves shown in these figures: as is already noted, both the hemolysis and the ionic-leakage curves show an approximately 1.5-fold span in field intensity. This indicates that different cells in the sample are pierced with the pores at different field intensities. The fact that this span is always about 1.5-fold, being independent of the ionic strength and the pulse duration, suggests a geometrical origin for the variance rather than a distribution in ΔV_c. A human erythrocyte has a shape of biconcave disk. According to Ponder [12], the diameter of the disk ranges between 8.5 ± 0.4 μm, the thickness at the maximum 2.4 ± 0.1 μm, and the volume 88 ± 6 μm^3. Therefore, the cell may be approximated by an oblate spheroid with an axial ratio ν of 0.28 (a = 4.3 μm, b = 1.2 μm, $(4\pi/3)a^2b$ = 93 μm^3). With this ν, the factor f in Eqn. 1 varies 1.4-fold (0.87—1.10) as θ_0, the orientation of the cell, changes between 0 and $\pi/2$ (Appendix I). Under a uniform electric field, therefore, ΔV_{max} in different cells is expected to range 1.5-fold, 1.4-fold being contributed from f and 1.1-fold from a. Thus, the experimentally observed span of 1.5-fold in the hemolysis and the ionic-leakage curves can be explained solely by the distribution of the orientation and the size of the cells in the sample. In other words, the critical transmembrane potential ΔV_c is the same for all the cells in the sample.

Now the value of this ΔV_c is estimated from an ionic-leakage curve as fol-

lows. The midpoint of this curve gives the field intensity $E_{1/2}$ at which 50% of the treated cells become leaky. The cell that is opened up at this very intensity is the one that is tilted from the direction of the field by θ_0 of $\pi/3$, because half of the total cells have θ_0 of less than $\pi/3$ while the other half above $\pi/3$ (the probability that a cell has an orientation between θ_0 and $\theta_0 + d\theta_0$ is proportional to $\sin \theta_0 d\theta_0$). Since $f(0.28, \pi/3) = 1.12$ (Appendix I), the critical transmembrane potential ΔV_c is obtained as

$$\Delta V_c \approx 1.1\, a E_{1/2} \tag{2}$$

For the typical pulse duration of 20 μs, ΔV_c is calculated to be 1.0 V. Values for other durations are obtained from the right-hand ordinate of Fig. 5.

Kinetics of the pore formation

Hemolysis reaction is accelerated by an increase either in the field intensity or the pulse duration, or by a reduction of the ionic strength of the pulsation medium. Any of these three changes, in other words, increase the rate of permeation of solute molecules across the cell membranes.

In general, either an expansion of the pore size or the formation of additional pores can account for the higher permeability. The previous study [8] has revealed, however, that the size limit for permeant molecules increases under the above conditions, indicating the widening of the pores. The present findings also support this view: a prolonged pulsation, for example, would increase the number of the pores if the time required for the formation of a pore is comparable to the pulse duration, or if the pores are created by a random process where the probability is proportional to time. Neither seems to be the case because the critical transmembrane potential is almost independent of the pulse duration (Fig. 5) and that doubling the duration more than doubles the rate of hemolysis in a range as wide as 10—320 μs (Table II, row 1). Likewise, it is difficult to assume that lowering the ionic strength would increase the number of pores, in view of the fact that the critical transmembrane potential remains the same (Fig. 3). Thus, the observed acceleration of hemolysis reaction is due mostly to an expansion of the pores.

In contrast to the pore size, the occurrence of the pores is determined solely by the magnitude of the transmembrane potential. The apparent increase in the critical transmembrane potential with very short pulses (Fig. 5) is attributed to the rise time (about 0.3 μs; see Appendix II) of the potential due to the membrane capacitance. Thus, the process of pore formation begins once the transmembrane potential reaches a critical value of about 1.0 V and is complete within a fraction of a microsecond. Further rise of the potential, or prolonged exposure only widens the pores; the low ionic strength facilitates this widening process, but not the initial process.

That the initial penetration is complete within 1 μs was directly confirmed by the following observation: when erythrocytes were pulsated at a low ionic strength, the current passing through the suspension increased with time, indicating the electrophoretic leakage of intracellular ions into the medium. Appreciable increases were observed only when the field intensity exceeded the critical value, and the uprise of current started within 1 μs of the front edge of the pulse.

Pore formation as a general response to a large transmembrane potential

Alteration of membrane permeability by a pulsed membrane potential at around 1 V has been observed in many cellular systems. Sale and Hamilton [1] showed lysis of a number of bacterial protoplasts and sphereoplasts as well as equine and bovine erythrocytes at critical transmembrane potentials ranging between 0.7 and 1.15 V. They attributed these lysis to the loss of semipermeable nature of cell membranes. Coster and Zimmermann [13], applying intracellular electrodes to *Valonia utricularis*, found a large and discontinuous decrease in the membrane impedance at a breakdown potential of 0.85 V; the membrane spontaneously resealed after 5 s, excluding the possibility of global damage. Decrease in membrane impedance at 1.1—1.4 V was also reported by Zimmermann et al. [14] for human and bovine erythrocytes and *Escherichia coli* B passing through the orifice of a Coulter counter. Neumann and Rosenheck [15] observed release of catecholamines and ATP, but not of proteins, from chromaffin granules at a pulsed electric field of 25 kV/cm, which corresponds to a maximum transmembrane potential of 0.45 V [16]. Rosenheck et al. [17] also reported that the release occurs within a few ms.

All the above phenomena appear to be consistent with the formation of pores in plasma membranes. In no cases has the total rupture of membrane been reported; the observed cell lysis is very likely colloid osmotic in nature. In several cases, the increased permeability has been confirmed to be limited to small molecules; release of intracellular proteins, where it was observed, is probably the result of colloid osmotic lysis. The sigmoidal dependence on the field intensity in all phenomena and the remarkably similar values of the critical transmembrane potential suggest a common mechanism of pore formation in all these systems.

The remaining problem is to elucidate the nature of the pores in molecular terms. Are they structural defects or lesions in lipid bilayers, or those involving proteins, existing ionic channels modified by the potential, or something else? And how does the potential induce the intra- or intermolecular structural change in membranes? Data available at present allow us to suggest that: (i) The number of molecules forming an initial pore must be small, probably one protein or several lipid molecules, since the limiting size for permeation is smaller than the size of a sucrose molecule. (ii) The effective pore size is continuously adjustable by the subsequent widening process to at least above the size of stachyose (average radius 0.6 nm) [8]. Thus, the entire process of the pore formation cannot be explained by a transition between two states, such as protein conformational change or dissociation in a single residue. (iii) The presence of the well-defined critical potential and the almost instantaneous (<1 μs) formation of the pores argue against the involvement of thermal processes such as local heating due to transmembrane current, although such processes may be important in the widening step. (iv) The effect of ionic strength suggests the presence of charged groups on, or around, the pore. However, the electrostatic force between these charges does not play a role in the initial process. (v) The pore is stable at 4°C, but reseals rapidly and completely at 37°C [8]. (vi) The mechanism is likely to be common to a variety of plasma membranes. Points (iii), (iv) and (vi) appear to favor the idea of dielectric breakdown [2,18], that occurs in a highly localized region(s), as the initial process of the pore formation, although its molecular implication is not necessarily clear.

Appendix I

Transmembrane potential in spheroidal cells

As shown in Fig. 6, we considere a spheroidal cell at the origin exposed to a uniform electric field E_0 lying in the x-z plane. Depending on whether the cell shape is oblate (axial ratio $\nu \equiv b/a < 1$) or prolate ($\nu \equiv 1$), we introduce oblate or prolate spheroidal coordinates (u, v, ϕ) such that

$$\begin{cases} (x^2 + y^2)^{1/2} = h(u^2 \pm 1)^{1/2}(1 - v^2)^{1/2} \\ z = huv \\ \tan^{-1}(y/x) = \phi \\ h = a|1 - \nu^2|^{1/2} \end{cases} \tag{1A}$$

(upper sign: oblate, lower sign: prolate)

whereupon the surface of the cell is represented by

$$u = a\nu/h \equiv c \tag{2A}$$

In the steady state, the electric potential V outside the cell satisfies Laplace's equation:

$$\nabla^2 V(u, v, \phi) = 0 \tag{3A}$$

Since the resistivity of plasma membranes (10—10^5 $\Omega \cdot cm^2$, corresponding to specific resistivity values of 10^7—10^{11} $\Omega \cdot cm$) is much higher than that of internal (approx. 200 $\Omega \cdot cm$) or external (approx. 100 $\Omega \cdot cm$ for isotonic saline) media [7,11], we can neglect the normal component of current at the surface of the cell, so that

$$[\partial V/\partial u]_{u=c} = 0 \tag{4A}$$

At a sufficiently long distance ($u \to \infty$) V takes the form:

$$\begin{aligned} V(u, v, \phi)_{u\to\infty} &= E_0(z \cos\theta_0 + x \cos\theta_0) \\ &= E_0 h[uv \cos\theta_0 + (u^2 \pm 1)^{1/2}(1 - v^2)^{1/2} \cos\phi \sin\theta_0] \end{aligned} \tag{5A}$$

Solving Eqn. 3A under the boundary conditions 4A and 5A, we obtain

$$V(u, v, \phi) = E_0 h[P(u)\, v \cos\theta_0 + Q(u)(1 - v^2)^{1/2} \cos\phi \sin\theta_0] \tag{6A}$$

where

$$\begin{cases} P(u) = u - \dfrac{u \cos^{-1}[u/(u^2+1)^{1/2}] - 1}{\cos^{-1}\nu - \nu(1-\nu^2)^{1/2}} \\ Q(u) = (u^2+1)^{1/2} - \dfrac{(u^2+1)^{1/2} \cos^{-1}[u/(u^2+1)^{1/2}] - u/(u^2+1)^{1/2}}{\cos^{-1}\nu - (2-\nu^2)(1-\nu^2)^{1/2}/\nu} \end{cases} \tag{7A}$$

for oblate, and

$$\begin{cases} P(u) = u - \dfrac{(u/2)\ln[(u+1)/(u-1)] - 1}{\ln[\nu + (\nu^2-1)^{1/2}] - \nu(\nu^2-1)^{1/2}} \\ Q(u) = (u^2-1)^{1/2} - \dfrac{[(u^2-1)^{1/2}/2]\ln[(u+1)/(u-1)] - u/(u^2-1)^{1/2}}{\ln[\nu + (\nu^2-1)^{1/2}] - (2-\nu^2)(\nu^2-1)^{1/2}/\nu} \end{cases} \tag{8A}$$

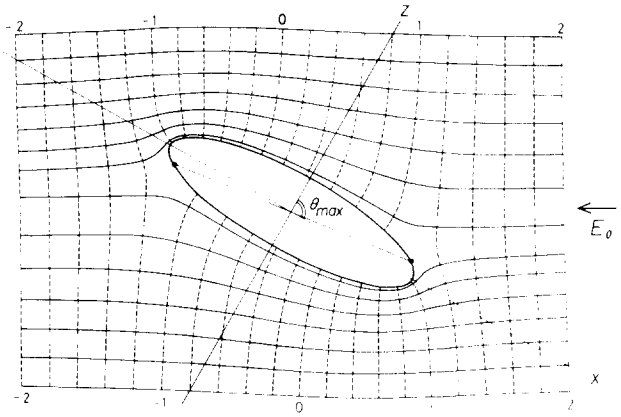

Fig. 7. Lines of current flow (solid lines) and equipotential surfaces (dashed lines) around an oblate spheroidal cell with an axial ratio of 0.28. Applied field in x-z plane makes an angle of $\pi/3$ with z-axis. The two dots on the cell surface show the points where the transmembrane potential becomes maximal. Potential values are in units of aE_0.

for prolate. An example of potential profile and the lines of current flow thus obtained is shown in Fig. 7 for the case of $\nu = 0.28$ and $\theta_0 = \pi/3$.

Since $V \equiv 0$ inside the cell under the assumption of zero membrane current, transmembrane potential ΔV is given simply by $V(u = c, v, \phi)$. The maximal transmembrane potential ΔV_{max} in particular, appears at two points (opposite signs) in the membrane, as shown in Fig. 7, the positions being given by θ_{max} such that

$$\tan \theta_{max} = [Q(c)/\nu P(c)] \tan \theta_0 \tag{9A}$$

The maximal value of ΔV_{max} is given by

$$\Delta V_{max} = E_0 h [P(c)^2 \cos^2\theta_0 + Q(c)^2 \sin^2\theta_0]^{1/2} \tag{10A}$$

The geometric factor f in Eqn. 1 in text is obtained by dividing ΔV_{max} with either $E_0 a$ (oblate) or $E_0 b$ (prolate). Note that these results are independent of the thickness of the membrane, which we have ignored, provided the conductivity of the membrane is low.

Numerical values of f as well as the position of the maximal potential θ_{max} are plotted in Fig. 8 against the axial ratio ν for several values of θ_0. The geometric factor f is greatest for a spherical cell, because distortion of the applied uniform field is maximal for the case of a sphere. For a given axial ratio ν, on the other hand, f becomes maximal when the largest semi-axis lies parallel to the direction of applied field. If cells are randomly oriented in a suspension, the median cell of the population has θ_0 of $\pi/3$, as has already been mentioned in text. Corresponding values of f and θ_{max} are shown in the figure.

Except the case of a sphere, θ_{max} always deviates from θ_0 in the direction approaching the largest semi-axis. The most probable site of the pore formation, therefore, is the rim of an ablate cell or the edge of a prolate cell.

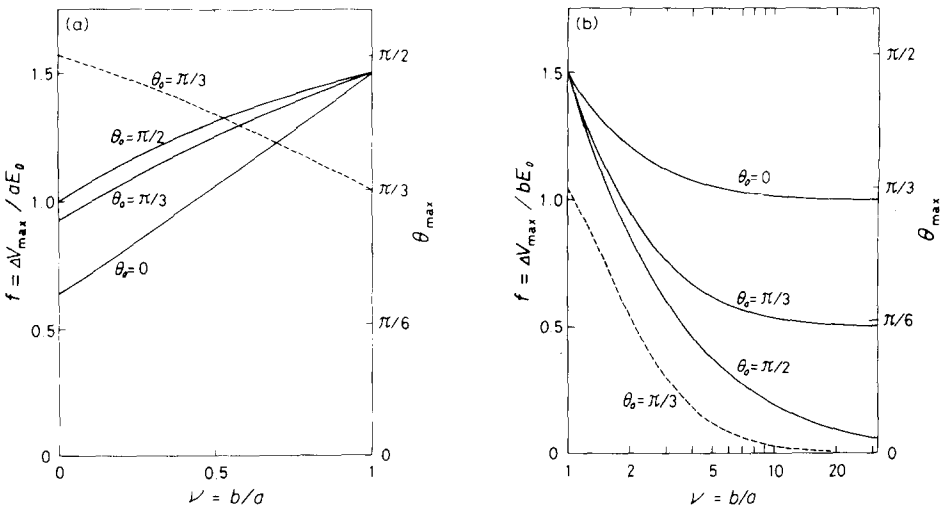

Fig. 8. The geometric factor f (solid lines) and the position of the maximal transmembrane potential θ_{max} (dashed lines) versus axial ratio $\nu = b/a$. Fig. 8a is for oblates, 8b for prolates. For symbols, refer to Figs. 6 and 7.

Appendix II

Rise time of the transmembrane potential

Here we consider, for the sake of simplicity, a spherical membrane of radius a separating internal and external fluids of resistivity r_i and r_e (subscripts i and e, hereafter, refer to internal and external spaces). At time $t = 0$, we apply a uniform electric field E_0 in the direction of $-z$. If we ignore the intrinsic membrane potential as well as the zeta potential arising from the fixed surface charges, both being in the order of 10 mV for human erythrocytes [7,19], the initial distribution of the electric potential V_i and V_e expressed in spherical coordinates is given by

$$V_i(r, \theta, \phi; t = 0) = V_e(r, \theta, \phi; t = 0) = E_0 r \cos\theta \tag{11A}$$

For $t \geqq 0$, since no electric charge accumulates in space other than the surfaces of the membrane, we obtain

$$\nabla^2 V_i(r, \theta, \phi; t) = \nabla^2 V_e(r, \theta, \phi; t) = 0 \tag{12A}$$

whereas the current component normal to the membrane surface accumulates ions to create surface charge densities q_i and q_e:

$$\begin{cases} \partial q_i(\theta, \phi; t)/\partial t = -(1/r_i)[\partial V_i/\partial r]_{r=a} \\ \partial q_e(\theta, \phi; t)/\partial t = (1/r_e)[\partial V_e/\partial r]_{r=a} \end{cases} \tag{13A}$$

Here, as in Appendix I, we have neglected the current passing through the membrane. We have also ignored the diffusional flow of ions [20], because we are dealing with a potential difference in the order of 1 V over the dimension of the cell (cf. thermal energy ≈ 0.026 eV). The charge densities are related with each other through the membrane capacitance C:

$$q_i = C(V_i - V_e)_{r=a} = -q_e \tag{14A}$$

Finally, the external potential satisfies the boundary condition:

$$V(r, \theta, \phi; t)_{r\to\infty} = r \cos\theta \tag{15A}$$

Solving Eqns. 11A—15A, we obtain:

$$V_i = E_0 r \cos\theta e^{-t/\tau} \quad \text{and} \quad V_e = E_0 r \cos\theta [1 + (a^3/2r^3)(1 - e^{-t/\tau})] \tag{16A}$$

$$\text{where} \quad \tau = aC(r_i + r_e/2) \tag{17A}$$

The transmembrane potential $\Delta V \equiv (V_e - V_i)_{r=a}$ approaches the steady-state value with τ as a time constant:

$$\Delta V = 1.5\, E_0 a \cos\theta(1 - e^{-t/\tau}) \tag{18A}$$

The expression 17A has been derived by Cole [21].

For an erythrocyte in isotonic saline, we may take $a = 3\ \mu m$, $C = 1\ \mu F/cm^2$, $r_i = 200\ \Omega \cdot cm$, and $r_e = 100\ \Omega \cdot cm$ [7,11,22], arriving at an estimated rise time τ of 0.1 μs. In the 10% NaCl/90% sucrose isotonic mixture, τ would be approx. 0.3 μs.

NOTE ADDED IN PROOF (received June 17th, 1977)

In the first row of Table I (ref. 8) the Na^+ and K^+ contents of erythrocytes before the voltage treatment were interchanged by mistake. Correct values should read 10 mmol $\cdot$ l^{-1} cells for Na^+, and 91 mmol $\cdot$ l^{-1} cells for K^+.

We are grateful to Dr. M.I. Kanehisa for his help in the calculation of potential profiles, to Mrs. K. Kinosita, Jr. for technical assistance, and to Professor J.L. Gamble, Jr. for allowing us to use his flame photometer. We are also indebted to Dr. T.T. Tsong for many helpful discussions. This work was supported by a grant from the United States Public Health Services.

References

1 Sale, A.J.H. and Hamilton, W.A. (1968) Biochim. Biophys. Acta 163, 37—43
2 Riemann, F., Zimmermann, U. and Pilwat, G. (1975) Biochim. Biophys. Acta 394, 449—462
3 Tsong, T.Y. and Kingsley, E. (1975) J. Biol. Chem. 250, 786—789
4 Tsong, T.Y., Tsong, T.T., Kingsley, E. and Siliciano, R. (1976) Biophys. J. 16, 1091—1104
5 Kinosita, Jr., K. and Tsong, T.Y. (1977) Proc. Natl. Acad. Sci. U.S. 74, 1923—1927
6 Wilbrandt, W. (1941) Pflüg. Arch. Ges. Physiol. 245, 22—52
7 Whittam, R. (1964) Transport and Diffusion in Red Blood Cells, Edward Arnold, London
8 Kinosita, Jr., K. and Tsong, T.Y. (1977) Nature 268, 438—441
9 Yoshida, S. and Ikegami, A. (1974) Biochim. Biophys. Acta 367, 39—46
10 Hoffman, J.F. (1973) Red Cell Shape (Bessis, M., Weed, R.I. and Leblond, P.F., eds.), pp. 51—54, Springer Verlag, New York
11 Cole, K.S. (1968) Membranes, Ions and Impulses, University of California Press, Los Angeles
12 Ponder, E. (1948) Hemolysis and Related Phenomena, Grune and Stratton, New York
13 Coster, H.G.L. and Zimmermann, U. (1975) Biochim. Biophys. Acta 382, 410—418
14 Zimmermann, U., Pilwat, G. and Riemann, F. (1974) Biophys. J; 14, 881—899
15 Neumann, E. and Rosenheck, K. (1972) J. Membrane Biol. 10, 279—290
16 Neumann, E. and Rosenheck, K. (1973) J. Membrane Biol. 14, 194—196
17 Rosenheck, K., Lindner, P. and Pecht, I. (1975) J. Membrane Biol. 20, 1—12
18 Crowley, J.M. (1973) Biophys. J. 13, 711—724
19 Lassen, U.V. and Stein-Knudsen, O. (1968) J. Physiol. 195, 681—696
20 Schwarz, G. (1962) J. Phys. Chem. 66, 2636—2642
21 Cole, K.S. (1937) Trans. Faraday Soc. 33, 966—972
22 Pauly, H. and Schwan, H.P. (1966) Biophys. J. 6, 621—639